The Journal of Supercritical Fluids 229 (2026) 106803

Contents lists available at ScienceDirect

The Journal of Supercritical Fluids

journal homepage: www.elsevier.com/locate/supflu

Valorisation of tomato peel waste for lycopene encapsulation: Optimization and comparison of two green techniques

Junyang Li [a], Chiara Bufalini [a], Stefania Mottola [b], Maria Chiara Iannaco [b], Roberta Campardelli [a,*], Iolanda De Marco [b,*]

[a] Department of Civil, Chemical and Environmental Engineering, University of Genoa, Via Opera Pia, 15, Genoa, 16145, Italy
[b] Department of Industrial Engineering, University of Salerno, Via Giovanni Paolo II, 132, Fisciano, Salerno, 84084, Italy

HIGHLIGHTS

- Lycopene was extracted from tomato waste and encapsulated in polycaprolactone (PCL).
- Use of two green methods: Supercritical Emulsion Extraction and Solvent Evaporation.
- Process optimization was done via Box-Behnken design and response surface modeling.
- Experimental validation confirmed the optimal conditions predicted by the DoE model.
- SEE showed more consistent encapsulation efficiency than solvent evaporation method.

GRAPHICAL ABSTRACT

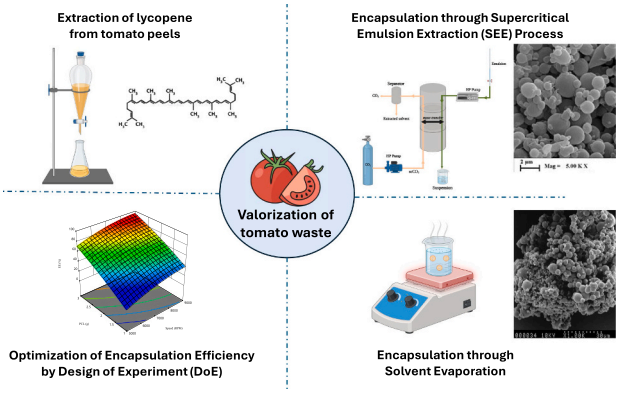

ARTICLE INFO

Keywords:
PCL
Microparticles production
DoE
Solvent evaporation
Supercritical emulsion extraction
Waste valorization

ABSTRACT

Lycopene, a lipid-soluble carotenoid with potent antioxidant properties, is typically found in tomato peels, which are often discarded as by-products in the food industry. This study focused on extracting lycopene using solvent extraction and encapsulating it in polycaprolactone (PCL), a biodegradable polymer, using two different methods: solvent evaporation and supercritical emulsion extraction (SEE). Both methods were used to produce microparticles for nutraceutical applications. An optimization study based on Box-Behnken design and response surface modelling was conducted to assess the effects of emulsification stirring speed, emulsification time, and polymer amount on encapsulation efficiency and particle size. Particle sizes, measured by laser diffraction, ranged between 1.77 ± 0.10 and 2.82 ± 0.17 μm for solvent evaporation, and between 1.12 ± 0.03 and 2.72 ± 0.15 μm for SEE. Encapsulation efficiencies, measured by UV–vis spectroscopy, ranged between 28.45 ± 0.28 % and 89.94 ± 1.70 % for solvent evaporation, and between 66.52 ± 0.64 % and 89.45 ± 1.31 % for SEE. Results show that SEE yields more consistent encapsulation efficiencies compared to solvent evaporation. Additionally, the design of experiments (DoE) approach helped identify optimal conditions that minimize waste and maximize productivity. This work offers a sustainable method for converting agro-industrial waste into valuable nutraceutical products.

* Corresponding authors.
E-mail addresses: roberta.campardelli@unige.it (R. Campardelli), idemarco@unisa.it (I. De Marco).

https://doi.org/10.1016/j.supflu.2025.106803
Received 29 July 2025; Received in revised form 7 October 2025; Accepted 8 October 2025
Available online 10 October 2025

1. Introduction

The food processing industry generates large quantities of by-products and waste at every stage each year. These materials represent an abundant, cost-effective, and renewable resource. Since typical food waste contains approximately 30–60 % starch, 10–40 % lipids, and 5–10 % proteins by weight, there is significant – yet underutilized – potential for nutrient recovery from both plant and animal sources [1]. The growth of the global tomato processing sector, largely driven by increasing demand for fresh and processed tomato products, has naturally resulted in a higher volume of by-products and waste. Studies show that tomato processing generates 30–40 % waste [2]. Proper disposal of this waste presents both economic and environmental challenges, as its low biological stability and microbial activity contribute to greenhouse gas emissions, exacerbating climate change [2]. In this context, repurposing agricultural and food industry by-products for nutrient recovery not only reduces waste but also supports Sustainable Development Goal 12.3, which aims to halve food waste and losses at all stages of the supply chain – including post-harvest – by 2030 [3].

Tomato by-products such as peels, seeds, and pomace are rich in fiber, polyphenols, carotenoids (including lycopene and β-carotene), oil, and proteins. These components offer notable health benefits due to their chemical and biological properties [4]. Lycopene is renowned for its strong antioxidant activity, which has been associated with the reduction of oxidative stress and the potential prevention of cancer, cardiovascular diseases, and neurodegenerative disorders [5,6].

In recent years, increased interest in healthy lifestyles has led to growing demand for functional nutrients and greater acceptance of alternative therapies. Lycopene, due to its promising properties, has become one of the most extensively studied bioactive compounds used in nutraceuticals [7,8]. However, lycopene remains underused because of its instability and low bioavailability [9]. Encapsulation can improve the stability of this compound, protecting it from degradation caused by light, oxygen, and heat, and thus extending its shelf life and enhancing its effectiveness [10,11]. Moreover, the right encapsulation strategy can increase solubility and enable controlled release [12].

Polymeric microparticles are a commonly used carrier for encapsulating lipophilic substances. The single oil-in-water emulsion solvent evaporation technique is typically used for the polymeric particles production [13–15]. In this method, the bioactive compound and polymer are dissolved in the oil phase, which is then dispersed into an aqueous phase containing a surfactant to stabilize the emulsion. Solvent removal from the oil phase results in the formation of polymeric particles. This method influences particle size, encapsulation efficiency, release characteristics, and the stability of the encapsulated compound [16]. Solvent evaporation is a fast process that usually occurs at room temperature, which is advantageous for preserving sensitive compounds such as enzymes [17]. However, it is generally a batch process, which limits productivity compared to continuous processes.

In recent years, supercritical fluids have gained attention as a medium for extracting organic solvents from the oil phase of emulsions. The supercritical emulsion extraction (SEE) method produces microparticles with a narrow size distribution and high encapsulation efficiency, while minimizing solvent residues and eliminating the need for a drying step [18,19]. Its mild operating conditions make it particularly suitable for thermolabile compounds, including essential oils, vitamins, and hydrophobic drugs [20,21]. Moreover, SEE can operate continuously, offering higher productivity compared to traditional batch processes.

The choice of polymer plays a crucial role in encapsulation performance. Poly(ε-caprolactone) (PCL) is a biodegradable and biocompatible polymer, approved for pharmaceutical use and obtainable from renewable resources. Its slow degradation rate makes it suitable for sustained release of lipophilic compounds such as lycopene [22]. PCL microparticles also offer high encapsulation efficiency and protect bioactive ingredients from oxidation. Furthermore, PCL is compatible with various other polymers and surfactants, increasing its versatility in nutraceutical applications [23,24].

Several studies in the literature have shown progress in encapsulating carotenoids, including lycopene, within PCL and other polymer matrices [25]. For example, PCL-based carriers are known to create nanoparticles that are smaller and have a slower erosion rate compared to poly(lactic-co-glycolic) acid [26]. Additionally, methoxy poly (ethylene glycol)-block-poly(ε-caprolactone) formulations of lycopene have demonstrated enhanced bioavailability and biological activity [27]. Lycopene has also been successfully encapsulated in PCL lipid-core nanocapsules, resulting in particles of approximately 190 nm with good stability [28]. Furthermore, earlier research has explored encapsulating carotenoids in polymeric carriers using the SEE process. Indeed, SEE has been employed to encapsulate astaxanthin in ethyl cellulose, resulting in particles of approximately 300 nm in diameter with a high encapsulation efficiency of 83 % [29]. Moreover, Santos et al. [30] reported the production of sub-micrometric particles of β-carotene and lycopene using the SEE process, achieving particles that are both highly stable and easily soluble in water.

To develop a process that not only transforms industrial waste into high-value nutraceutical ingredients but also enhances efficiency, a statistical methodology such as Design of Experiments (DoE) can be employed. DoE combined with response surface methodology (RSM) allows for a systematic investigation of the relationships between input variables and outcomes [31]. In this study, factors such as polymer concentration, emulsification time and stirring speed were evaluated to determine their influence on product quality and yield. Once optimal conditions are identified, the process becomes easier to standardize and control, thereby reducing variability [32]. DoE also contributes to sustainability by identifying process conditions that maximize efficiency while minimizing environmental impact, such as energy, water, and solvent use.

Building on these considerations, the primary objective of this work was to extract lycopene from tomato peels, an agro-industrial waste, and used it to produce particles that enable the creation of a stable lycopene formulation suitable for nutraceutical applications. Two different encapsulation techniques, emulsion solvent evaporation and supercritical emulsion extraction (SEE), were compared to produce microparticles. The effects of polymer concentration, emulsification time, and emulsification stirring speed were investigated with respect to particle morphology and encapsulation efficiency. A Box-Behnken design was applied to optimize the experimental process, and the effects of different process variables were systematically studied using response surface modeling (RSM). The overall aim of this study was to promote sustainability and support the circular economy by transforming food waste into valuable resources, while also highlighting the environmental and quality-related benefits of the supercritical encapsulation method.

2. Materials and methods

2.1. Chemicals

Tomato waste (peels and seeds) was kindly provided by a producer of tomato sauce in northern Italy. Poly(ε-caprolactone) (average Mn ~ 14000 g/mol) (PCL) was purchased from Sigma-Aldrich (Saint Louis, MO, USA). Polysorbate 80 (Tween 80) was purchased from Acros Organics (Geel, Belgium). Chloroform was purchased from Carlo Erba (Milan, Italy). Carbon Dioxide was purchased from Morlando Group (Naples, Italy). Distilled water was produced with lab-scale equipment in our laboratory.

2.2. Lycopene extraction from tomato waste

The extraction of lycopene was performed using chloroform through conventional solid-liquid extraction, following the methodology reported by Rozzi et al. [33], with minor modifications. The tomato waste was partially dried at 60°C up to a constant weight before the extraction.

The extraction was conducted using a liquid-to-solid ratio of 10 mL/g at room temperature (25 °C), with an extraction time of 12 h, using a magnetic stirrer and in the dark. The extraction vessel used had an internal volume of 500 mL. The obtained enriched lycopene extract was characterized in terms of total lycopene concentration, which was evaluated by measuring the absorbance at 470 nm using a UV–vis spectrophotometer (Lambda 25, PerkinElmer, Wellesley, MA, USA) [34]. The used calibration curve is reported in Eq. 1.

$$C_{TL} = 7.2884 \quad \times Abs \tag{1}$$

where C_{TL} is the total lycopene concentration expressed as milligrams of equivalent lycopene per milliliter of extract (mg_{LE}/mL) and Abs is the absorbance at the wavelength of 470 nm.

2.3. Emulsion preparation

To prepare the oil-in-water emulsion (O/W), the oil phase (O) was obtained by adding PCL to the lycopene extracted from tomato peels; in particular, 1–3 g of PCL were added to 20 g of extract constituted by chloroform rich in lycopene. The water phase (W) was prepared by dissolving Tween 80 at a concentration of 1 % (*w/w*). The mass ratio between the oil and the water phase was fixed at 20/80, and 100 g of emulsion was produced for each batch. Different emulsification stirring speeds (5000 – 9000 rpm), and emulsification times (3 – 9 min) were tested. Moreover, various amounts of PCL as the carrier agent were investigated. These different quantities were reported as PCL weight percentage, defined as the mass of PCL (ranging from 1 to 3 g) relative to the total mass of the oil phase (fixed at 20 g). The emulsion production was carried out using a Silverson L5M-A rotor-stator type emulsifier (Silverson Machines Ltd, Chesham, UK). All the processes were conducted in an ice bath to prevent a possible degradation of the compounds due to high temperatures.

2.4. Production of polymeric particles with emulsion solvent evaporation method

The loaded polymer particles were produced using the solvent evaporation method. Specifically, the emulsions were mixed at 200 rpm at room temperature (25 ± 2°C) to allow complete solvent evaporation, which, for a 100 mL batch, corresponds to approximately 8 h. The obtained particle suspension was centrifuged at 11760 ×g for 10 min. Then, the particles were resuspended in pure water and recovered by filtration (membrane filters 0.22 μm, Millipore, Burlington, MA, USA). Unloaded particles were also produced without the addition of lycopene extract in the oil phase.

2.5. Production of polymeric particles with supercritical emulsion extraction (SEE)

The oil-in-water emulsions were also processed using the SEE plant, schematically represented in a previous work [35]. The setup consists of a 1.6-meter-high column with an internal diameter of 13 mm. The column is divided into four cylindrical sections, connected by cross-shaped unions. The interior was packed with stainless steel structured packing (0.16-inch ProPak, Scientific Development Company, State College, PA) characterized by a void fraction of 0.94, to assure phase contact and mass transfer efficiency under the selected operating conditions. The column is thermally insulated with a fiberglass jacket, and the temperature profile is controlled by six temperature controllers along the column (Series 93, Watlow, Milan, Italy).

In each SEE experiment, CO_2 is supplied to the bottom of the column at a constant flow rate via a high-pressure pump (Milroyal B, Milton Roy, Pont Saint Pierre, France), while the emulsion is fed into the top of the column using a high-pressure piston pump (Model 305, Gilson, France). The extracted oily phase is collected in a separator located downstream of the column's top, while the particle suspension is continuously recovered at the column's bottom through decompression using a needle valve. In the case of SEE, the processing time is 90 min for a 100 mL batch. Operating conditions were selected based on previous studies, with an emulsion flow rate of 2.4 mL/min, a fixed liquid-to-gas mass ratio of 0.1, and temperature and pressure set at 37°C and 80 bar [36]. The pressure value was chosen to ensure lycopene insolubility in supercritical carbon dioxide, thus preventing its extraction [37]. Solid particles were recovered from the suspension using the same treatment method as in the conventional process.

2.6. Experimental design

Response Surface Methodology (RSM) was used to adapt the Box-Behnken design to tune the preparation of particles for both the investigated techniques [38]. The independent variables for optimization were selected as follows: emulsification stirring speed as factor 1 (X_1), emulsification time as factor 2 (X_2), and PCL weight percentage as factor 3 (X_3). The selected responses were particle mean Sauter diameter (D_{32}) and encapsulation efficiency of lycopene (EE). Each independent variable was given a high- and low-level value for a total of 15 runs, in which the central point was performed in triplicate (Table 1). The experimental data were mathematically fitted through a second-order polynomial (Eq. 2):

$$Y = a_0 + \sum_{i=1}^{k} a_i X_i + \sum_{i=1}^{k} a_{ii} X_i^2 + \sum_{i=1}^{k} \sum_{j=1}^{k} a_{ij} X_i X_j \tag{2}$$

where Y are response variables, X_i and X_j are the input variables, a_0 is a constant, a_i, a_{ii}, and a_{ij} are the coefficients of the linear, quadratic, and interaction terms of the equation, respectively. The model adequacy was determined by the analysis of variance (ANOVA) using the Design Expert Software (Stat-Ease, Inc., Minneapolis, MN, USA).

2.7. Physicochemical characterization

2.7.1. Polymeric particles morphology

The morphology of polymeric particles was observed using field emission scanning electron microscopy (FESEM, LEO 1525, Carl Zeiss SMT AG, Oberkochen, Germany), equipped with a secondary electron detector, used with a 10 kV voltage. Samples were placed on a carbon tab previously fixed to an aluminum stub (Agar Scientific, Stansted, UK) and then coated with gold-palladium (layer thickness 25 nm) using a sputtering coater (108 A, Agar Scientific, Stansted, UK).

2.7.2. Particle size analysis

The produced particles were analyzed using a laser diffraction particle size analyzer (Mastersizer 3000, Malvern Instruments Ltd, Worcestershire, UK) for particle size distribution (PSD) using the methods described by Ushikubo & Cunha [39] with slight modifications. Briefly, the samples were dispersed in deionized water up to a laser obscuration between 10 % and 20 %. All measurements were performed in triplicate, and the polymeric particles were characterized by Sauter mean diameter

Table 1
Main chart of Box-Behnken design for the production of polymeric microparticles.

Independent variables		Emulsification stirring speed X_1 [rpm]	Emulsification time X_2 [min]	PCL weight percentage X_3 [g]
Level	Low	5000	3	5
	High	9000	9	15
Dependent variables		D_{32} [μm]	EE [%]	

(D_{32}).

2.7.3. Encapsulation efficiency

The encapsulation efficiency (EE) was evaluated by analyzing the total and free lycopene content in the particles and comparing them to the initially loaded lycopene, following the procedure adapted from Zhao et al. [40]. To determine the total lycopene content, 1 mL of the particle suspension was dissolved in 3 mL of chloroform and vortexed for 1 min to release the lycopene from the produced particles. A particle suspension without lycopene was used as a control.

For the free lycopene content, 1 mL of the particle suspension was dissolved in 3 mL of acetone and shaken for 1 min. The solid was then separated by centrifugation at 4000 rpm for 10 min to obtain the acetone phase.

Both total and free lycopene contents were measured by evaluating absorbance (Abs) using a UV-Vis spectrophotometer (Lambda 25, PerkinElmer, Wellesley, MA, USA) at 470 nm, based on the calibration curve reported in Eq. 1 [40].

The encapsulation efficiency (EE) was calculated by the following Eq. 3:

$$EE = \frac{m_{total} - m_{free}}{m_{loaded}} \quad x \quad 100 \tag{3}$$

Where m_{total} was the mass of total lycopene, m_{free} was the mass of free lycopene, and m_{loaded} was the mass of initial loaded lycopene.

2.7.4. Dissolution tests

Lycopene dissolution tests were conducted using a Cary 60 UV/vis spectrophotometer at a wavelength of 475 nm. To compare dissolution rates, samples with the highest encapsulation efficiency, obtained by the solvent evaporation method and the SEE method were selected. Both samples, weighing 30 mg each, were placed in a porous paper filter and incubated in a 50/50 v/v acetone/water solution. The mixture was continuously stirred at 200 rpm and maintained at 37 °C. The absorbance was continuously monitored throughout the release process with Kinetics software until all the lycopene was released into the medium. The final release percentage was then calculated by comparing the initial and final absorbance values at the plateau.

3. Results and discussion

3.1. Extract production and characterization

To ensure a lycopene-rich extract, tomato waste was subjected to chloroform extraction at a solid-to-liquid ratio of 1:10, following a protocol reported in the literature. The obtained extract was characterized by a concentration of lycopene equal to 176.76 μg/mL in the final extract.

3.2. Experimental design of polymeric particles production by emulsion solvent evaporation

Polymeric particles are a potential carrier for the encapsulation of lycopene-rich extract. Due to the strong lipophilicity of lycopene, the emulsion solvent evaporation technique was investigated as producing technique. The response surface methodology was used to investigate the effect of process parameters and to optimize the production. A total of 15 experimental runs were carried out in order to study the effect of three independent variables, i.e. emulsification stirring speed (X_1), emulsification time (X_2), and PCL weight percentage (X_3). Each experimental run was characterized in terms of particles mean diameter (D_{32}) and encapsulation efficiency (EE). The values of the input variables in the considered design space points and the experimental results, in terms of response variables, are presented in Table 2.

All the performed tests successfully produced polymeric microparticles with a mean diameter D_{32} between 1.77 ± 0.10 and 2.82 ± 0.17 μm. The particle size distributions (PSDs) of particles with lower and higher D_{32} (Run 7 and Run 15) are shown in Fig. 1 as an example. It was possible to see that the PSDs were unimodal and uniform, indicating a good particle homogeneity. Moreover, the SEM images of all the experiments are reported in Fig. 2 and it can be seen that the microparticles obtained were well-formed and spherical in all the conditions investigated.

Regarding the mean diameter of polymeric particles (D_{32}), it was modeled according to a reduced quadratic model (Eq. 4) and analysis of variance (ANOVA) was performed (Table 3) to assess the significance of the model and equation terms.

The model was characterized by a F – value of 52.89 and a p – value lower than 0.0001 (Table 3), meaning that there is less than 0.01 % of probability that such a large F – value will occur due to noise. The p – values less than 0.05 (Table 3) show that the model terms were significant. This indicated that the model was highly significant for the fitting of particle diameter. Moreover, the goodness of fit was also checked by the good coefficient of determination ($R^2 = 0.9570$). The predicted R^2 value (0.8987) was reasonably in agreement with the adjusted one (0.9570). The signal-to-noise ratio was satisfactory since the observed good precision ratio of 23.508 was greater than 4. In addition, the coefficient of variation (CV = 2.86 %) calculated from the replicates at the central point showed good experimental precision. Therefore, this model could be used to represent the design space studied. Looking at the actual equation (Eq. 4), the coded coefficients (Tables 3) and 3D surface plots (Fig. 3), it is evident that the particle diameter was predominantly affected by factor X_3, representing the polymer concentration, which exhibited the largest positive effect. This means that increasing the polymer concentration significantly increased the particle size. This behavior is commonly observed in polymer particle production, where a higher amount of polymer raises the viscosity of the dispersed phase, reducing the effectiveness of shear forces during emulsification and leading to larger particles [41–43]. Considering the emulsion solvent evaporation technique, the particle diameter was correlated to the operating conditions of the emulsification process, in terms of speed and time. In particular, the speed had a negative coefficient, indicating that higher homogenization speeds resulted in smaller particle sizes. As reported in the literature [44,45], increasing the homogenization speed enhances shear force and turbulence, promoting droplet breakup and reducing the average particle diameter. The emulsification time showed a positive effect, suggesting that prolonged emulsification might favor coalescence or limit further droplet size reduction beyond a certain duration. The interaction term between X_1 and X_3 was also statistically significant and revealed a critical relationship between emulsification speed and polymer concentration. As also shown in Fig. 3B, the efficiency of stirring is affected by the viscosity of the liquid, which increases with higher polymer content. In more viscous systems, even high stirring speeds may not translate into effective shear stress, thus limiting droplet breakup. This interaction reflects a typical phenomenon in emulsion-based systems, where the effectiveness of mechanical forces is modulated by the rheological properties of the liquid phases.

$$D_{32} = - \quad 0.35 + 0.000409 \quad X_1 + 0.17 \quad X_2 + 0.13 \quad X_3 \\ - 0.000010 \quad X_1X_3 - 2.87 * 10^{-8} X_1^2 \quad - 0.011 \quad X_2^2 \tag{4}$$

The encapsulation efficiency was between 28.45 ± 0.28 and 89.94 ± 1.70 %, highlighting a great variability depending on the different process parameters. The encapsulation efficiency (EE) was modeled according to a reduced quadratic model (Eq. 5) and analysis of variance (ANOVA) was performed (Table 4) to assess the significance of the model and equation terms.

The analysis of variance (ANOVA) showed a F – value of 106.10 and a p – value less than 0.0001 (Table 4), indicating an excellent overall

Table 2
Values of the input variables (X_1: emulsification stirring speed; X_2: emulsification time, X_3: PCL weight percentage) in the Box-Behnken design of the polymeric particles production process, and experimental results of the response variables (D_{32}: mean diameter of polymeric particles, EE: encapsulation efficiency) for particles produced by the emulsion solvent evaporation and supercritical emulsion extraction methods. Data are reported as mean value of triplicate analyses ± standard deviation.

Run	Factor			Response for emulsion solvent evaporation		Response for supercritical emulsion extraction	
	X_1 [rpm]	X_2 [min]	X_3 [%]	D_{32} [μm]	EE [%]	D_{32} [μm]	EE [%]
1	9000	9	10	2.11 ± 0.35	70.34 ± 0.52	1.81 ± 0.04	87.13 ± 1.93
2	5000	9	10	2.56 ± 0.15	43.41 ± 0.65	1.31 ± 0.04	75.76 ± 0.53
3	5000	3	10	2.18 ± 0.43	73.52 ± 0.41	2.72 ± 0.15	72.12 ± 1.35
4	7000	9	15	2.69 ± 0.78	89.94 ± 1.70	1.12 ± 0.03	87.78 ± 0.86
5	7000	6	10	2.40 ± 0.32	66.81 ± 0.54	1.50 ± 0.04	82.55 ± 0.53
6	7000	6	10	2.36 ± 0.09	65.95 ± 1.15	1.55 ± 0.07	78.18 ± 0.82
7	7000	3	5	1.77 ± 0.10	78.63 ± 0.19	1.19 ± 0.06	69.99 ± 0.39
8	9000	6	15	2.19 ± 0.27	68.06 ± 0.43	1.68 ± 0.06	89.45 ± 1.31
9	9000	3	10	1.9 ± 0.33	62.12 ± 0.61	1.94 ± 0.03	80.32 ± 0.82
10	7000	3	15	2.45 ± 0.10	59.76 ± 0.51	1.81 ± 0.02	84.87 ± 0.99
11	5000	6	5	2.05 ± 0.09	45.17 ± 0.64	1.18 ± 0.04	66.52 ± 0.64
12	9000	6	5	1.84 ± 0.76	54.66 ± 0.29	1.36 ± 0.06	76.23 ± 0.82
13	7000	6	10	2.46 ± 0.14	65.47 ± 0.20	1.43 ± 0.01	81.46 ± 1.11
14	7000	9	5	2.07 ± 0.08	28.45 ± 0.28	1.23 ± 0.02	72.45 ± 1.03
15	5000	6	15	2.82 ± 0.17	63.04 ± 0.72	1.83 ± 0.05	81.43 ± 0.49

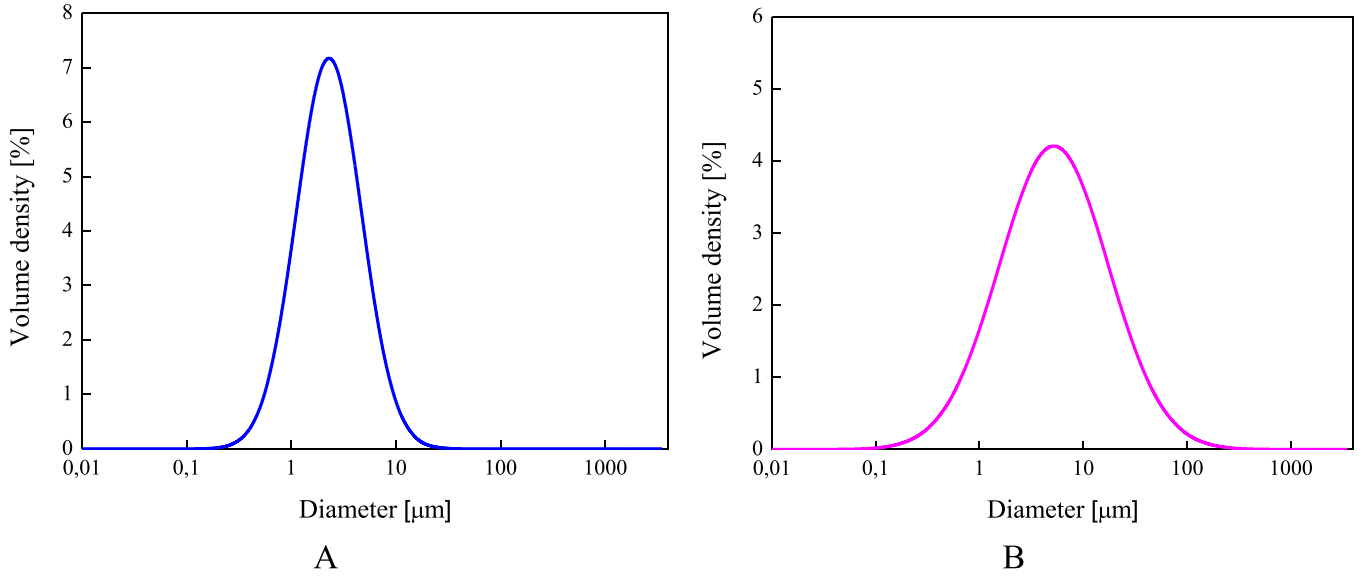

Fig. 1. Particle size distribution (PSD) for polymeric particles of Run 7 (A) and Run 15 (B) for the emulsion solvent evaporation method.

model fit. The coefficient of determination (R^2 = 0.9907) further confirmed the model's strong agreement with the experimental data, explaining most of the variability in the response variable. In addition, the similarity between the predicted R^2 (0.9441) and the adjusted R^2 (0.9813) suggested the model had good predictive ability and a low risk of overfitting. Furthermore, the signal-to-noise ratio of the model reached 39.120, well above the recommended minimum of 4. This provides further evidence of the model's robustness and reliability. Looking at the actual equation (Eq. 5) and at the coded coefficients (Table 4), the encapsulation efficiency was predominantly affected by factors X_3, $X_1 \times_2$, and $X_2 \times_3$. Among the linear effects, X_3 showed the positive impact, indicating that increasing the quantity of carrier material enhances the availability of wall matrix for the encapsulation of lycopene, thereby improving the overall encapsulation efficiency [46]. On the other hand, emulsification time had a negative linear effect, suggesting that prolonged emulsification may negatively affect the encapsulation process, while emulsification speed contributed positively. The positive interaction between X_2 and X_3 was the most influential among the interaction terms, indicating a synergistic effect: when adequate emulsification time is combined with enough polymer, the encapsulation process is significantly enhanced. Additionally, the interaction between X_1 and X_2 ($X_1 \times_2$) also contributed positively, suggesting that under certain conditions, increasing both speed and time could support more efficient particle formation. The presence of significant negative quadratic effects for X_1^2 and X_3^2 indicates that further increases in emulsification speed or polymer concentration may lead to decreased encapsulation efficiency, possibly due to excessive shear or unfavorable viscosity and particle aggregation. These results are consistent with the trends observed in the 3D response surface plots (Fig. 4), which illustrate how the combined effects of the process parameters influence the system's behavior.

$$EE = 116.06 + 0.011 \quad X_1 - 26.32 \quad X_2 - 3.51 \quad X_3 + 0.0016 \quad X_1X_2 + 1.34 \quad X_2X_3 - 1.30 * 10^{-6} X_1^2 - 0.134 \quad X_3^2 \tag{5}$$

After studying the effect of the process parameters on the responses (D_{32} and EE), the optimum values of the input variables in order to obtain the maximum encapsulation were found. The optimized operating conditions were: 7422 rpm, 8.978 min, and 14.992 %. The

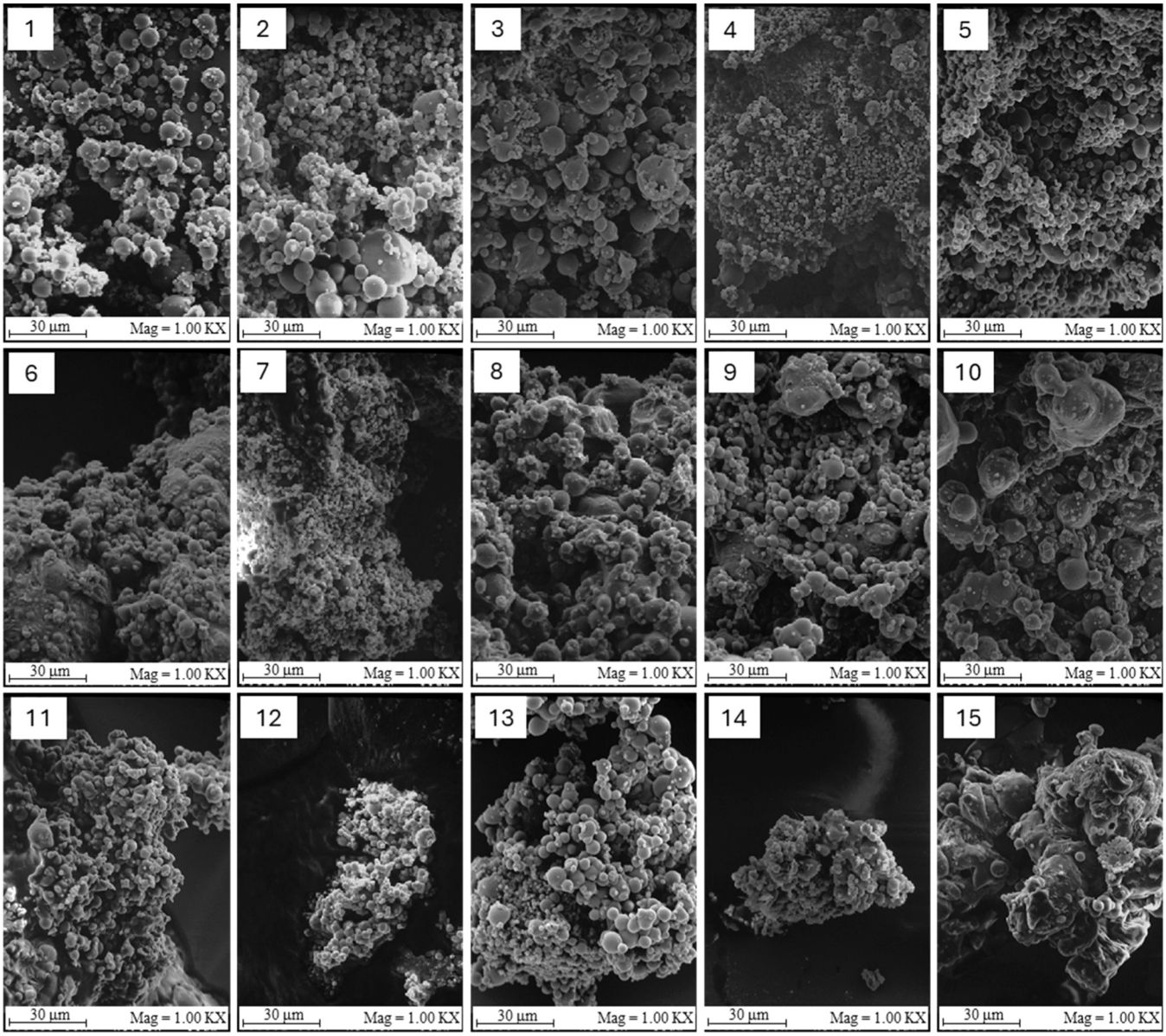

Fig. 2. SEM images of particles produced using emulsion solvent evaporation method at each run described in Table 2.

Table 3
Coded coefficients for Eq. 4 and statistical analysis results of ANOVA of the fitted reduced quadratic polynomial model for particles diameter (D_{32}) for emulsion solvent evaporation method.

Source	Coded coefficient	Sum of square	Mean of square	F – value	p – value
Model		1.32	0.2201	52.89	< 0.0001
Intercept	+ 2.37				
X_1	- 0.1963	0.3081	0.3081	74.03	< 0.0001
X_2	+ 0.1412	0.1596	0.1596	38.35	0.0003
X_3	+ 0.3025	0.7321	0.7321	175.88	< 0.0001
$X_1 \times_3$	- 0.1050	0.0441	0.0441	10.60	0.0116
X_1^2	- 0.1148	0.0490	0.04090	11.76	0.0090
X_2^2	- 0.0948	0.0334	0.0334	8.02	0.0221
Residual		0.0333	0.0042		
Lack of Fit		0.0282	0.0047	1.86	0.3905

obtained optimal point was experimentally verified, and the produced particles were characterized by a D_{32} of 2.69 ± 0.50 µm and an EE of 89.95 ± 0.83 %. These results showed a good agreement with the prediction, highlighting the validity of the model.

3.3. Experimental design of polymeric particles production by supercritical emulsion extraction (SEE)

The same emulsions were processed using supercritical emulsion extraction to remove chloroform from the oil phase. The performed experiments and the corresponding results are summarized in the last two columns of Table 2.

The results presented in Table 2 show that the SEE process produced microparticles with a mean diameter (D_{32}) ranging from 1.12 ± 0.03 and 2.72 ± 0.15 µm. The particle size distributions (PSDs) for runs 7 and 15 (Fig. 5) clearly demonstrate that this method enables effective control over particle size, resulting in unimodal and uniform distributions. Furthermore, Fig. 6 shows SEM images from all tests, demonstrating the attainment of spherical, well-shaped microparticles across all tests performed using the SEE process.

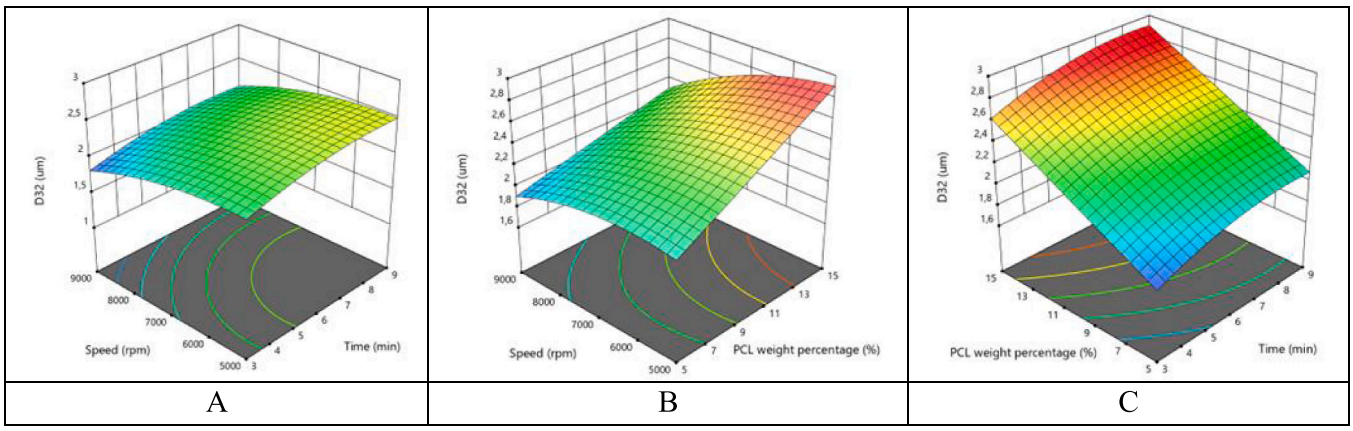

Fig. 3. 3D surface plots for particle diameter as a function of emulsification stirring speed and emulsification time for 10 % as PCL weight percentage (A), emulsification stirring speed and PCL weight percentage for 9 min as emulsification time (B), and emulsification time and PCL weight percentage for 5000 rpm as emulsification stirring speed (C) in the case of emulsion solvent evaporation method.

Table 4
Coded coefficients for Eq. 5 and statistical analysis results of ANOVA of the fitted reduced quadratic polynomial model for encapsulation efficiency (EE) for the emulsion solvent evaporation method.

Source	Coded coefficient	Sum of square	Mean of square	F – value	p – value
Model		3129.72	447.10	106.10	< 0.0001
Intercept	+ 66.92				
X_1	+ 3.76	112.8	112.8	26.77	0.0013
X_2	- 5.24	219.36	219.36	52.05	0.0002
X_3	+ 9.24	682.3	682.3	161.91	< 0.0001
$X_1 \times_2$	+ 9.58	367.29	367.29	87.16	< 0.0001
$X_2 \times_3$	+ 20.09	1614.22	1614.22	383.06	< 0.0001
X_1^2	- 5.20	100.53	100.53	23.86	0.0018
X_3^2	- 3.35	41.78	41.78	9.92	0.0162
Residual		29.50	4.21		
Lack of Fit		28.58	5.72	12.51	0.0757

The mean diameter of polymeric particles (D_{32}) was modeled using a reduced quadratic model (Eq. 6), and an analysis of variance (ANOVA) was performed (Table 6) to assess the significance of the model and its terms. The model exhibited a F – value of 17.14 and a p – value of 0.0007 (Table 6), indicating that the probability of obtaining this result by random noise is less than 0.07 %. The significance of the model terms was confirmed by p-values less than 0.05 (Table 6), further supporting the relevance of the selected variables. These results demonstrate that the model is highly significant for fitting particle diameter data.

Furthermore, the reliability of the model was validated by the high coefficient of determination ($R^2 = 0.9449$), suggesting an excellent fit. The adequacy of the signal-to-noise ratio was confirmed by a precision value of 13.579, which exceeds the minimum acceptable threshold of 4. A low coefficient of variation (CV = 9.39 %) also reflects high experimental precision.

Overall, the statistical parameters confirm that the model (Eq. 6) is well-suited to describe the studied design space. The effect of the input variables on particle size is shown by the coded coefficients (Table 6) and illustrated in the 3D response surface plots in Fig. 7. Regarding the emulsification stirring speed, the linear term of X_1 was not statistically significant, while the quadratic term (X_1^2) was significant, indicating a nonlinear effect of emulsification speed on particle size. This suggests the existence of an optimal value of X_1, beyond which further increases may no longer reduce the droplet size and could even lead to an increase. Moreover, as shown in Fig. 7A, the smallest values of diameter are obtained at high levels of both emulsification speed (X_1) and emulsification time (X_2). In contrast, emulsification time (X_2) showed a significant positive linear effect, and its interaction with polymer concentration (X_2X_3) further influenced the response. Increasing the amount of polymer (X_3) led to an increase in particle diameter, likely due to the higher viscosity of the dispersed phase, which affects the initial droplet formation and, consequently, the final microparticle size [47].

$$D_{32}{}^{-1.3} = -0.53 + 0.000506X_1 + 0.077X_2 - 0.077X_3 - 0.000016X_1X_2 + 0.0072X_2X_3 - 2.99 * 10^{-8} \quad X_1^2 + 0.0055 \quad X_3^2 \tag{6}$$

The encapsulation efficiency, a key parameter in this study, ranged from 66.52 ± 0.64 % to 89.45 ± 1.31 % when the SEE process was used. These values were slightly higher than those obtained with the solvent evaporation in the initial part of the study. Although lycopene is a non-polar compound known to be soluble in supercritical CO_2, the chosen operating conditions in this study ensured that extraction did not occur. This confirms that under the selected conditions, supercritical CO_2 did not interfere with the active compound or affect the encapsulation process [36].

Encapsulation efficiency was described using a linear model (Eq. 7), and its reliability was verified through ANOVA (Table 7). The statistical evaluation revealed a high F-value of 81.38 and a p-value < 0.0001, confirming the model's statistical significance. The coefficient of determination ($R^2 = 0.9569$) indicated that the model has a good predictive ability. Additionally, the predicted R^2 (0.9355) agreed with the adjusted R^2 (0.9451), demonstrating that the model offers accurate

Table 5
Comparison of predicted values and experimental responses of the optimized operating conditions for the emulsion solvent evaporation method. The operating conditions were approximated for the experimental evaluation.

Parameters	Goal	Importance	Experimental operation conditions	Predicted value	Observed value	Prediction error [%]
X_1 [rpm]	In range	3	7400			
X_2 [min]	In range	3	9			
X_3 [%]	In range	3	15			
D_{32} [μm]	In range	3		2.649	2.69 ± 0.50	1.55
EE [%]	Maximize	5		90.072	89.95 ± 0.83	0.10

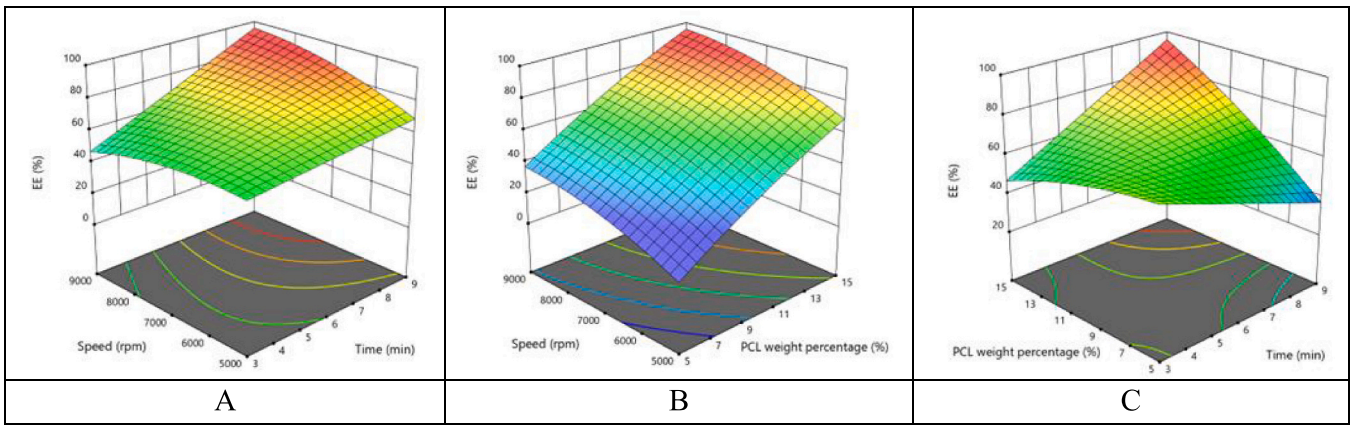

Fig. 4. 3D surface plots for encapsulation efficiency as function of emulsification stirring speed and emulsification time for 15 % as PCL weight percentage (A), emulsification stirring speed and PCL weight percentage for 9 min as emulsification time (B), and emulsification time and PCL weight percentage for 9000 rpm as emulsification stirring speed (C) in the case of emulsion solvent evaporation method.

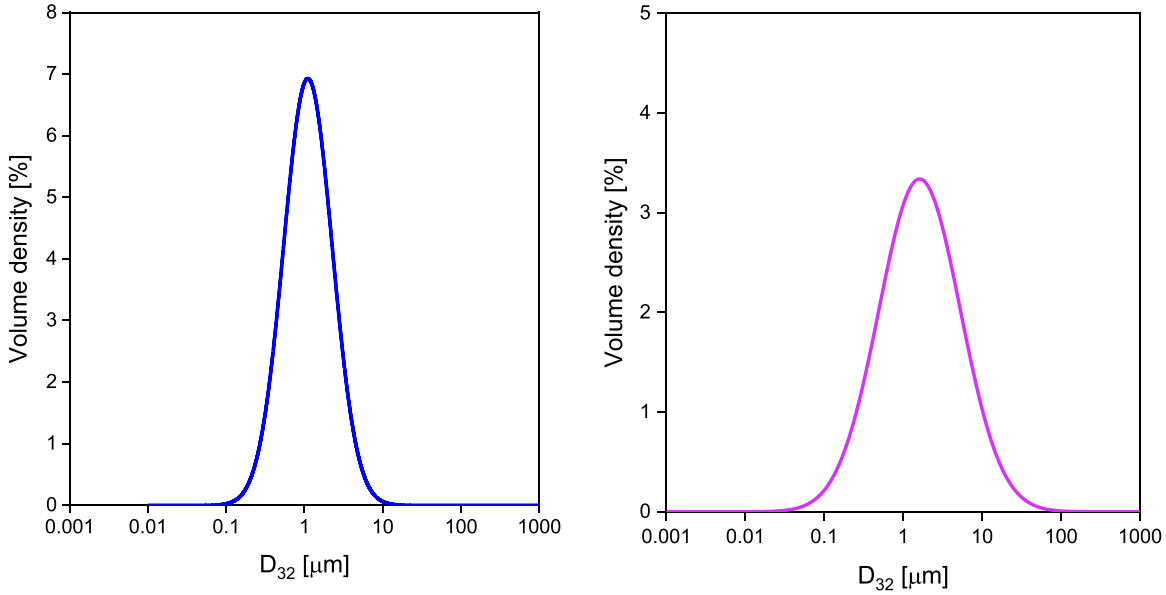

Fig. 5. Particle size distributions (PSDs) for SEE-processed particles obtained by Run 7 (A) and Run 15 (B) for SEE process.

predictions without signs of overfitting. The precision of the model was also supported by an adequate signal-to-noise ratio of 28.809, well above the acceptable threshold of 4, further validating the model's robustness. Based on the coefficients in the actual equation (Eq. 7) and the coded coefficients (Table 7), the variables with the greatest influence on EE were X_1 (emulsification stirring speed) and X_3 (PCL weight percentage). Eq. 7 and Fig. 8 illustrate the impact of input variables on encapsulation efficiency. Specifically, the coded coefficient for X_3 is notably the largest among the linear terms, indicating that increasing the polymer concentration has the most substantial positive effect on EE. This enhancement can be attributed to the increased availability of polymer matrix material, which facilitates the formation of a more effective encapsulating barrier around the active compound, thus improving its entrapment efficiency [48]. Additionally, the emulsification stirring speed (X_1) also positively affects EE. Higher emulsification speed contributes to improved encapsulation efficiency by producing more uniform and stable microparticles [49]. These effects are clearly shown in Fig. 8, indicating that increasing polymer concentration and emulsification stirring speed leads to improved encapsulation efficiency.

$$EE = 44.22 + 0.0023X_1 + 0.66X_2 + 1.46X_3 \quad (7)$$

Also in this case, the optimum values of the input variables in order to obtain the maximum encapsulation were found and they are 8429 rpm, 8.821 min, and 14.481 %. The experimental verification produced particles that were optimized with a D_{32} of 1.45 ± 0.11 μm and an EE of 92.13 ± 1.4 % (Table 8). Consequently, the validity of the model was also verified for the SEE process.

3.4. Comparison between solvent evaporation and supercritical emulsion extraction

Both investigated emulsion-based processes successfully encapsulated lycopene in polymeric microparticles. Furthermore, the conducted study identified the optimal operating conditions to maximize encapsulation efficiency. When the optimized operating conditions were compared, the input variable values were similar for both techniques, indicating that the initial emulsions were well formed and stable enough to allow particle production. Examining the predicted and observed values of the analyzed responses revealed that the encapsulation efficiency was high for both techniques. However, the SEE process exhibited a significant lower mean diameter, from 2.69 ± 0.50 μm to 1.45 ± 0.11 μm.

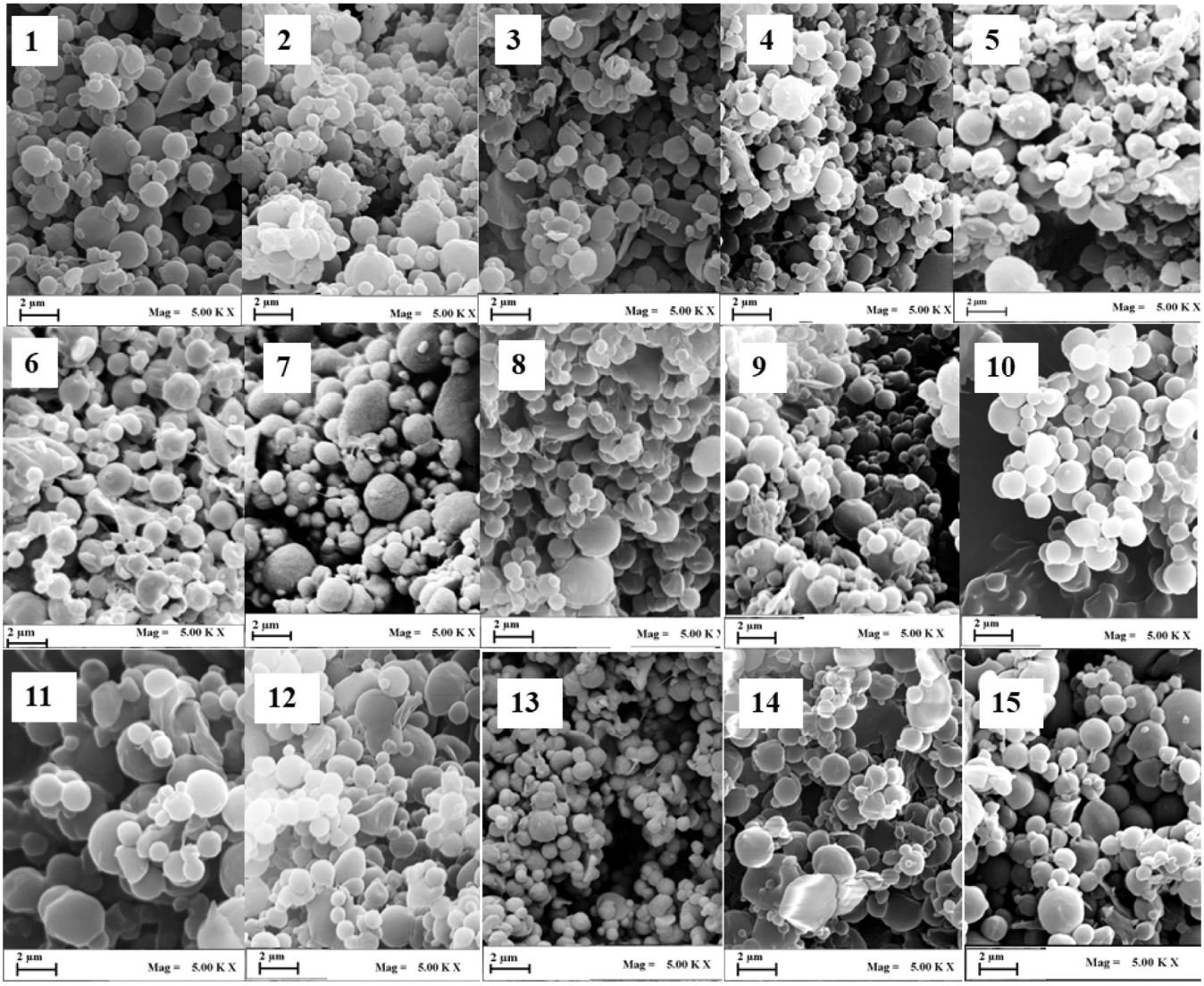

Fig. 6. FESEM images for all the runs for the SEE process.

Table 6
Coded coefficient referred to Eq. 6 and statistical analysis results of ANOVA of the fitted quadratic polynomial model for particles diameter (D_{32}) for SEE process.

Source	Coded coefficient	Sum of square	Mean of square	F – value	p – value
Model		0.3791	0.0542	17.14	0.0007
Intercept	+ 0.5891				
X_1	- 0.0217	0.0038	0.0038	1.19	0.3109
X_2	+ 0.1048	0.0879	0.0879	27.82	0.0012
X_3	- 0.0935	0.0699	0.0699	22.13	0.0022
$X_1 \times_2$	- 0.0979	0.0384	0.0384	12.14	0.0102
$X_2 \times_3$	+ 0.1085	0.0471	0.0471	14.91	0.0062
X_1^2	- 0.1196	0.0531	0.0531	16.82	0.0046
X_3^2	+ 0.1369	0.0696	0.0696	22.02	0.0022
Residual		0.0221	0.0032		
Lack of Fit		0.0201	0.0010	4.07	0.2091

To understand whether the emulsion processing method affects the lycopene release from the obtained particles, the dissolution rates were evaluated using the samples obtained by solvent evaporation and SEE which gave the best results in terms of encapsulation efficiency. The drug dissolution profiles reported in Fig. 9 show the percentage of lycopene dissolved in a 50/50 v/v acetone and water mixture over time.

The curves are quite similar in shape. Notably, for the SEE-processed sample, the release occurs slightly faster initially, reaching 80 % in just 20 min, while the solvent evaporation sample reaches 80 % release in 40 min. Both samples demonstrate a second, slower phase, and 100 % of the lycopene in both samples was released in approximately 100 min.

In conclusion, while both techniques are effective for lycopene encapsulation, supercritical emulsion extraction is more advantageous for controlling particle size, which is an important aspect for pharmaceutical or nutraceutical applications where bioavailability is strongly influenced by particle size. Essentially, in the SEE process, supercritical CO_2 rapidly extracts the organic solvent from the dispersed phase, leading to instantaneous precipitation of the active ingredient and polymer particles; the rapid precipitation limits the possibility of coalescence and agglomeration, as the particles quickly solidify before they can coalesce or aggregate. In contrast, when an emulsion is treated with solvent evaporation, the solvent removal process is much slower, giving the suspended particles time to aggregate or partially coalesce.

4. Conclusions

In conclusion, this study has explored the extraction of lycopene from tomato peels, a common by-product of the food industry, and its

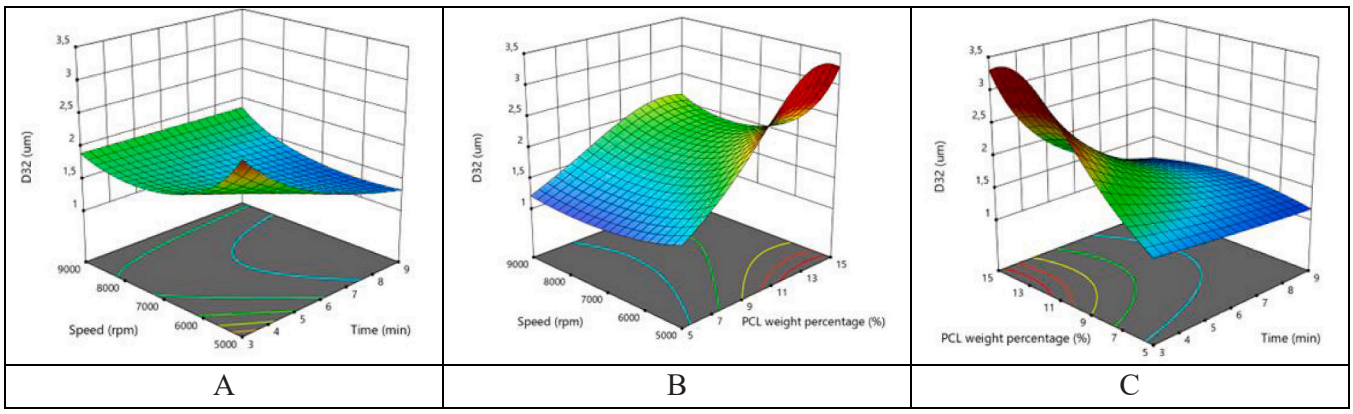

Fig. 7. 3D surface plots for particle diameter as a function of emulsification stirring speed and emulsification time for 10 % as PCL weight percentage (A), emulsification stirring speed and PCL weight percentage for 3 min as emulsification time (B), and emulsification time and PCL weight percentage for 5000 rpm as emulsification stirring speed (C) in the case of SEE process.

Table 7
Coded coefficients referred to Eq. 7 and statistical analysis results of ANOVA of the fitted quadratic polynomial model for encapsulation efficiency (EE) for SEE process.

Source	Coded coefficient	Sum of square	Mean of square	F – value	p – value
Model		630.64	210.21	81.38	< 0.0001
Intercept	+ 79.08				
X_1	+ 4.66	173.91	173.91	67.33	< 0.0001
X_2	+ 1.98	31.28	31.28	12.11	0.0051
X_3	+ 7.29	425.44	425.44	164.70	< 0.0001
Residual		28.41	2.58		
Lack of Fit		18.07	2.01	0.3880	0.8697

subsequent encapsulation in polycaprolactone (PCL) using two distinct methods: emulsion solvent evaporation and supercritical emulsion extraction (SEE).

Optimization revealed that key factors such as emulsification stirring speed, emulsification time, and polymer quantity significantly influenced both particle size and encapsulation efficiency.

Laser diffraction analysis confirmed that SEE produced smaller and more uniform particles (ranging from 1.12 ± 0.03 to 2.72 ± 0.15 μm) compared to the solvent evaporation method, which yielded particles between 1.77 ± 0.10 and 2.82 ± 0.17 μm, as also highlighted at the optimal point.

Encapsulation efficiencies also showed a marked improvement with SEE, showing more consistent results in the range 66.52 ± 0.64 % to 89.45 ± 1.31 %, compared to the more variable efficiencies obtained with solvent evaporation (28.45 ± 0.28 % to 89.94 ± 1.70 %). These findings underscore the superior potential of the SEE process in

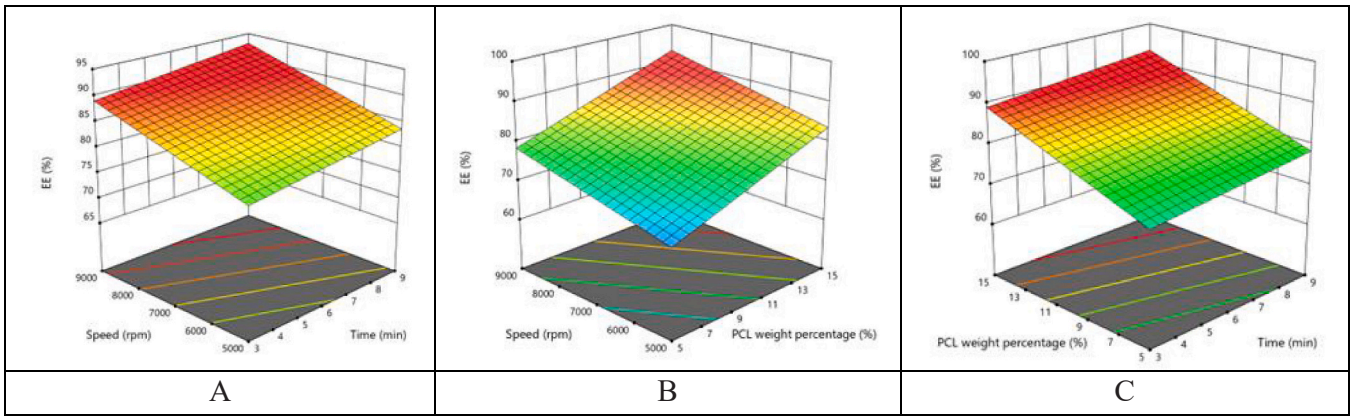

Fig. 8. 3D surface plots for encapsulation efficiency as a function of emulsification stirring speed and emulsification time for 15 % as PCL weight percentage (A), emulsification stirring speed and PCL weight percentage for 9 min a emulsification time (B), and emulsification time and PCL weight percentage for 9000 rpm as emulsification stirring speed (C) in the case of SEE process.

Table 8
Comparison of predicted values and experimental responses of the optimized operating conditions for SEE process. The operating conditions were approximated for the experimental evaluation.

Parameters	Goal	Importance	Experimental operation conditions	Predicted value	Observed value	Prediction error [%]
X_1 [rpm]	In range	3	8400			
X_2 [min]	In range	3	9			
X_3 [%]	In range	3	15			
D_{32} [μm]	In range	3		1.372	1.45 ± 0.11	5.70
EE [%]	Maximize	5		90.809	92.13 ± 1.4	1.45

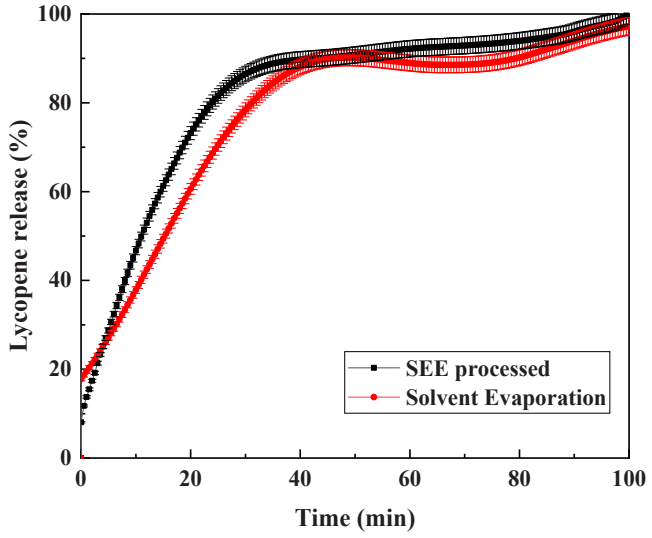

Fig. 9. Release curves of lycopene from solvent evaporation and SEE microparticles.

achieving high-quality encapsulation, along with the advantage of continuous operation. Moreover, the optimization approach not only reduced waste but also enhanced overall process productivity.

This study highlights the potential of using agro-industrial waste, such as tomato peels, for the sustainable production of nutraceutical products, presenting a promising avenue for waste valorization and improved resource efficiency in the food industry.

CRediT authorship contribution statement

Iolanda De Marco: Writing – review & editing, Supervision, Resources, Project administration, Funding acquisition, Data curation, Conceptualization. **Maria Chiara Iannaco:** Writing – original draft, Investigation, Formal analysis, Data curation. **Roberta Campardelli:** Writing – review & editing, Supervision, Resources, Project administration, Funding acquisition, Data curation, Conceptualization. **Stefania Mottola:** Writing – original draft, Validation, Methodology, Formal analysis, Data curation. **Junyang Li:** Writing – original draft, Investigation, Formal analysis, Data curation. **Chiara Bufalini:** Writing – original draft, Validation, Methodology, Formal analysis, Data curation.

Declaration of Competing Interest

The authors declare that they have no known competing financial interests or personal relationships that could have appeared to influence the work reported in this paper.

Data availability

Data will be made available on request.

References

[1] T.M. Hicks, C.J.R. VerbeekProtein-rich by-products: production statistics, legislative restrictions, and management options, in: Protein Byproducts: Transformation from Environmental Burden Into Value-Added Products, 2016, pp. 3-20..
[2] A. Rajan, S. Kumar, C.K. Sunil, M. Radhakrishnan, A. Rawson, Recent advances in the utilization of industrial byproducts and wastes generated at different stages of tomato processing: status report, J. Food Process. Preserv 46 (2022), https://doi.org/10.1111/jfpp.17063.
[3] O. Sylvester, Sustainable development goal 12: sustainable consumption and production patterns. in: Handbook on Public Policy and Food Security, Edward Elgar Publishing, 2024, pp. 289–298.
[4] V.N. Madia, D. De Vita, D. Ialongo, V. Tudino, A. De Leo, L. Scipione, R. Di Santo, R. Costi, A. Messore, Recent advances in recovery of lycopene from tomato waste: a potent antioxidant with endless benefits, Molecules 26 (2021), https://doi.org/10.3390/molecules26154495.
[5] E. Giovannucciomato products, lycopene, and prostate cancer: a review of the epidemiological literature, in: Journal of Nutrition, 2005, pp. 2030S-2031S.
[6] X. Liang, C. Ma, X. Yan, X. Liu, F. Liu, Advances in research on bioactivity, metabolism, stability and delivery systems of lycopene, Trends Food Sci. Technol. 93 (2019) 185–196, https://doi.org/10.1016/j.tifs.2019.08.019.
[7] M. Grabowska, D. Wawrzyniak, K. Rolle, P. Chomczyński, S. Oziewicz, S. Jurga, J. Barciszewski, Let food be your Medicine: nutraceutical properties of lycopene, Food Funct. 10 (2019) 3090–3102, https://doi.org/10.1039/c9fo00580c.
[8] D. Dutta, D. DuttaLycopene as nutraceuticals, in: Handbook of Nutraceuticals and Natural Products, 2022, pp. 205-243..
[9] H. Wu, Y. Wu, Z. Cui, L. Hu, Nutraceutical delivery systems to improve the bioaccessibility and bioavailability of lycopene: a review, Crit. Rev. Food Sci. Nutr. 64 (2024) 6361–6379, https://doi.org/10.1080/10408398.2023.2168249.
[10] M. Bakhshizadeh, T.N. Moghaddam, M. Tavassoli, A. Mousavi Khaneghah, E. Ansarifar, Characterization, extraction, and encapsulation technologies of lycopene and applications in functional food products: an updated review, Food Bioproc. Technol. 18 (2025) 3059–3099, https://doi.org/10.1007/s11947-024-03585-9.
[11] G.C. Carvalho, B.A.F. de Camargo, J.T.C. de Araújo, M. Chorilli, Lycopene: from tomato to its nutraceutical use and its association with nanotechnology, Trends Food Sci. Technol. 118 (2021) 447–458, https://doi.org/10.1016/j.tifs.2021.10.015.
[12] Y. Li, Y. Zhao, H. Zhang, Z. Ding, J. Han, The application of natural carotenoids in multiple fields and their encapsulation technology: a review, Molecules 29 (2024), https://doi.org/10.3390/molecules29050967.
[13] S. Banasaz, K. Morozova, G. Ferrentino, M. Scampicchio, Encapsulation of lipid-soluble bioactives by nanoemulsions, Molecules 25 (2020), https://doi.org/10.3390/molecules25173966.
[14] Z. Teixeira, N. Durán, S.S. Guterres, Annatto polymeric microparticles: natural product encapsulation by the emulsion-solvent evaporation method, J. Chem. Educ. 85 (2008) 946–947, https://doi.org/10.1021/ed085p946.
[15] A. Kumar, U. Singh, S.G. Jaiswal, J. Dave, S. Wei, G.G. Hailu, Recent trends in the encapsulation of functional lipids: comprehensive review, Sustain. Food Technol. 2 (2024) 1610–1630, https://doi.org/10.1039/d4fb00205a.
[16] N. Choudhury, M. Meghwal, K. Das, Microencapsulation: an overview on concepts, methods, properties and applications in foods, Food Front 2 (2021) 426–442, https://doi.org/10.1002/fft2.94.
[17] C. Ge, C. LiDong, X. ChunLi, Z. PengYue, C. Chong, L. FengMin, H. QiLiang, Performance study of prothioconazole microcapsules prepared by solvent evaporation method, Sci. Agric. Sin. 54 (2021) 754–767, https://doi.org/10.3864/j.issn.0578-1752.2021.04.008.
[18] H. Park, Exploring the effects of process parameters during W/O/W emulsion preparation and supercritical fluid extraction on the protein encapsulation and release properties of PLGA microspheres, Pharmaceutics 16 (2024), https://doi.org/10.3390/pharmaceutics16030302.
[19] I. Palazzo, E.P. Lamparelli, M.C. Ciardulli, P. Scala, E. Reverchon, N. Forsyth, N. Maffulli, A. Santoro, G. Della Porta, Supercritical emulsion extraction fabricated PLA/PLGA micro/nano carriers for growth factor delivery: release profiles and cytotoxicity, Int. J. Pharm. 592 (2021), https://doi.org/10.1016/j.ijpharm.2020.120108.
[20] D.F. Tirado, A. Latini, L. Calvo, The encapsulation of hydroxytyrosol-rich olive oil in Eudraguard® protect via supercritical fluid extraction of emulsions, J. Food Eng. 290 (2021), https://doi.org/10.1016/j.jfoodeng.2020.110215.
[21] D. Cerro, A. Torres, J. Romero, C. Streitt, A. Rojas, S. Matiacevich, S. Machuca, Supercritical fluid extraction of emulsion-assisted encapsulation of hypocholesterolemic bioactive compounds, J. Supercrit. Fluids 211 (2024), https://doi.org/10.1016/j.supflu.2024.106306.
[22] R.M. Mohamed, K. Yusoh, A review on the recent research of polycaprolactone (PCL), Adv. Mater. Res. 1134 (2015) 249–255, https://doi.org/10.4028/www.scientific.net/amr.1134.249.
[23] F. Taghizadeh, M. Heidari, S. Mostafavi, S.M. Mortazavi, A. Haeri, A review of preparation methods and biomedical applications of poly(ε-caprolactone)-based novel formulations, J. Mater. Sci. 59 (2024) 10587–10622, https://doi.org/10.1007/s10853-024-09774-3.
[24] N.S. Grewal, U. Batra, K. Kumar, A. Mahapatro, Novel PA encapsulated PCL hybrid coating for corrosion inhibition of biodegradable mg alloys: a triple triggered self-healing response for synergistic multiple protection, J. Magnes. Alloy 11 (2023) 1440–1460, https://doi.org/10.1016/j.jma.2023.01.019.
[25] M.T. Arshad, S. Maqsood, A. Ikram, A.A. Khan, A. Raza, A. Ahmad, K.T. Gnedeka, Encapsulation techniques of carotenoids and their multifunctional applications in food and health: an overview, Food Sci. Nutr. 13 (2025) e70310, https://doi.org/10.1002/fsn3.70310.
[26] M.A.U. Alam, L.S. Kassama, Comparative study of lycopene encapsulation efficiency in polycaprolactone vs poly lactic co-glycolic acid, in: 2019 ASABE Annual International Meeting, , ASABE, St. Joseph, MI, 2019, p. 1.
[27] S. Yin, X. Xu, Y. Li, H. Fang, J. Ren, Lycopene as a potential anticancer agent: current evidence on synergism, drug delivery systems and epidemiology (Review), Oncol. Lett. 30 (2025) 1–20, https://doi.org/10.3892/ol.2025.15208.
[28] P.P. dos Santos, K. Paese, S.S. Guterres, A.R. Pohlmann, T.H. Costa, A. Jablonski, S. H. Flôres, Ad.O. Rios, Development of lycopene-loaded lipid-core nanocapsules: physicochemical characterization and stability study, J. Nanopart. Res. 17 (2015) 107, https://doi.org/10.1007/s11051-015-2917-5.
[29] D.F. Tirado, I. Palazzo, M. Scognamiglio, L. Calvo, G. Della Porta, E. Reverchon, Astaxanthin encapsulation in ethyl cellulose carriers by continuous supercritical

emulsions extraction: a study on particle size, encapsulation efficiency, release profile and antioxidant activity, J. Supercrit. Fluids 150 (2019) 128–136, https://doi.org/10.1016/j.supflu.2019.04.017.
[30] D.T. Santos, Á. Martín, M.A.A. Meireles, M.J. Cocero, Production of stabilized submicrometric particles of carotenoids using supercritical fluid extraction of emulsions, J. Supercrit. Fluids 61 (2012) 167–174, https://doi.org/10.1016/j.supflu.2011.09.011.
[31] S. Beg, S. Swain, M. Rahman, M.S. Hasnain, S.S. Imam, Application of design of experiments (DoE) in pharmaceutical product and process optimization (, in:), Pharm. Qual. Des. Princ. Appl. (2019) 43–64.
[32] S. N. Politis, P. Colombo, G. Colombo, D. M. Rekkas, Design of experiments (DoE) in pharmaceutical development, Drug Dev. Ind. Pharm. 43 (2017) 889–901, https://doi.org/10.1080/03639045.2017.1291672.
[33] N.L. Rozzi, R.K. Singh, R.A. Vierling, B.A. Watkins, Supercritical fluid extraction of lycopene from tomato processing byproducts, J. Agric. Food Chem. 50 (2002) 2638–2643, https://doi.org/10.1021/jf011001t.
[34] J. Li, R. Campardelli, G. Firpo, J. Zhang, P. Perego, Oil-in-water nanoemulsions loaded with lycopene extracts encapsulated by spray drying: formulation, characterization and optimization, Chin. J. Chem. Eng. 70 (2024) 73–81, https://doi.org/10.1016/j.cjche.2024.03.002.
[35] R. Campardelli, E. Reverchon, G.Della PortaBiopolymer particles for proteins and peptides sustained release produced by supercritical emulsion extraction, in: Procedia Engineering, 2012, pp. 239-246.
[36] C. Gimenez-Rota, I. Palazzo, M.R. Scognamiglio, A. Mainar, E. Reverchon, G. Della Porta, B-Carotene, A-tocoferol and rosmarinic acid encapsulated within PLA/PLGA microcarriers by supercritical emulsion extraction: encapsulation efficiency, drugs shelf-life and antioxidant activity, J. Supercrit. Fluids 146 (2019) 199–207, https://doi.org/10.1016/j.supflu.2019.01.019.
[37] J. Shi, M. Khatri, S.J. Xue, G.S. Mittal, Y. Ma, D. Li, Solubility of lycopene in supercritical CO2 fluid as affected by temperature and pressure, Sep. Purif. Technol. 66 (2009) 322–328, https://doi.org/10.1016/j.seppur.2008.12.012.
[38] J. Li, M. Pettinato, A.A. Casazza, P. Perego, A comprehensive optimization of ultrasound-assisted extraction for lycopene recovery from tomato waste and encapsulation by spray drying, Processes 10 (2022), https://doi.org/10.3390/pr10020308.
[39] F.Y. Ushikubo, R.L. Cunha, Stability mechanisms of liquid water-in-oil emulsions, Food Hydrocoll. 34 (2014) 145–153, https://doi.org/10.1016/j.foodhyd.2012.11.016.
[40] C. Zhao, L. Wei, B. Yin, F. Liu, J. Li, X. Liu, J. Wang, Y. Wang, Encapsulation of lycopene within oil-in-water nanoemulsions using lactoferrin: impact of carrier oils on physicochemical stability and bioaccessibility, Int. J. Biol. Macromol. 153 (2020) 912–920, https://doi.org/10.1016/j.ijbiomac.2020.03.063.
[41] N. Innocente, M. Biasutti, E. Venir, M. Spaziani, G. Marchesini, Effect of high-pressure homogenization on droplet size distribution and rheological properties of ice cream mixes, J. Dairy Sci. 92 (2009) 1864–1875, https://doi.org/10.3168/jds.2008-1797.
[42] F. Lince, D.L. Marchisio, A.A. Barresi, Strategies to control the particle size distribution of poly-ε-caprolactone nanoparticles for pharmaceutical applications, J. Colloid Interface Sci. 322 (2008) 505–515, https://doi.org/10.1016/j.jcis.2008.03.033.
[43] M.D.P. Cavalcante, L.R. de Menezes, Effects of polycaprolactone viscosity on morphology, mechanical properties, water uptake, and cellular viability in poly(3-hydroxybutyrate)/polycaprolactone blends for tissue engineering, Polym. Adv. Technol. 35 (2024), https://doi.org/10.1002/pat.6224.
[44] T. Lemenand, P. Dupont, D.D. Valle, H. Peerhossaini, Comparative efficiency of shear, elongation and turbulent droplet breakup mechanisms: review and application, Chem. Eng. Res. Des. 91 (2013) 2587–2600, https://doi.org/10.1016/j.cherd.2013.03.017.
[45] T. Dapčević Hadnadev, P. Dokić, V. Krstonošić, M. Hadnadev, Influence of oil phase concentration on droplet size distribution and stability of oil-in-water emulsions, Eur. J. Lipid Sci. Technol. 115 (2013) 313–321, https://doi.org/10.1002/ejlt.201100321.
[46] S. Salatin, J. Barar, M. Barzegar-Jalali, K. Adibkia, F. Kiafar, M. Jelvehgari, Development of a nanoprecipitation method for the entrapment of a very water soluble drug into eudragit RL nanoparticles, Res. Pharm. Sci. 12 (2017) 1–14, https://doi.org/10.4103/1735-5362.199041.
[47] I. Palazzo, G. Viscusi, G. Gorrasi, E. Reverchon, Composite nanocapsules of phase change materials using a supercritical carbon dioxide (SC-CO2) assisted process, Can. J. Chem. Eng. 103 (2025) 1723–1735, https://doi.org/10.1002/cjce.25472.
[48] A. Gharsallaoui, G. Roudaut, O. Chambin, A. Voilley, R. Saurel, Applications of spray-drying in microencapsulation of food ingredients: an overview, Food Res. Int. 40 (2007) 1107–1121, https://doi.org/10.1016/j.foodres.2007.07.004.
[49] H.A. Zahran, G. Catalkaya, H. Yenipazar, E. Capanoglu, N. Şahin-Yeşilçubuk, Determination of the optimum conditions for emulsification and encapsulation of echium oil by response surface methodology, ACS Omega 8 (2023) 28249–28257, https://doi.org/10.1021/acsomega.3c01779.